Transducer sensitivity compensation using diagonal preconditioning for time reversal and Tikhonov inverse filtering in acoustic systems

Pierre M. Dumuid, Ben S. Cazzolato, and Anthony C. Zander
ANVC Group, School of Mechanical Engineering, The University of Adelaide, South Australia 5005

(Received 30 March 2005; revised 12 October 2005; accepted 13 October 2005)

Filters are commonly used in sound reproduction and communication systems as a means of compensating for the response of the electro-acoustic plant. Two commonly used filter designs in the field of acoustics are the time reversal filter and the Tikhonov inverse filter. In this paper the influence of transducer sensitivities on the performance of these filters is examined. It is shown that the sensitivity of the transducers can negatively affect the performance of the resulting filter. To compensate for the decrease in performance, diagonal preconditioning can be implemented in the system. It is shown that by using diagonal matrices, which minimize the condition number of the system, the loss in performance arising from unbalanced sensitivities is minimized. This paper proposes an algorithm to find such a set of diagonal matrices and results are presented showing the improvements in performance arising from the modified filter design. © *2006 Acoustical Society of America.* [DOI: 10.1121/1.2139069]

PACS number(s): 43.60.Pt, 43.60.−c, 43.38.Md [TDM] Pages: 372–381

I. INTRODUCTION

The control of transmissions through electro-acoustic systems has been an active topic of research for many years. Transmission through a system generally involves the design of a filter that manipulates input signals, such that when the output signals from the filter are transmitted through the physical system, the input signals are reproduced at the receiver. The design of such a filtering system depends on the type of physical system. The types of physical systems examined in this paper are multi-channel linear time-invariant (LTI) systems. Various designs of such filters exist for multi-channel LTI systems. Of particular interest in this work is that of designing a filter from measured impulse response functions (IRFs) of the system.[1–5] Two such filter designs are time reversal filters and Tikhonov inverse filters. When designing such filters, it is important to understand the influences various components of the system have on the resulting filter. A typical system contains a set of sensitivities for the transmitting and receiving elements. In this paper, it is shown that the choice of transducer sensitivity has a considerable influence on the resulting filters. This paper examines this influence for both time reversal and Tikhonov inverse filter designs. An algorithm is then given that generates more appropriate transducer sensitivities, and results are presented showing the improvement to the system performance.

II. BACKGROUND THEORY

The design of the multi-channel filter discussed in this paper is based on the system presented in Fig. 1. This figure shows input signals, $\mathbf{u}(z)$, transformed by the filter, $\mathbf{A}(z)$, to produce a set of signals, $\mathbf{d}(z)$, that are desired to be replicated by the signals, $\mathbf{w}(z)$, being the output of the electro-acoustic system denoted by $\mathbf{C}(z)$. In order to achieve this, a filter $\mathbf{H}(z)$ is designed based on $\mathbf{C}(z)$ and $\mathbf{A}(z)$. In general, the transfer matrix $\mathbf{A}(z)$ is a delay [i.e., $\mathbf{A}(z)=z^{-m}\mathbf{I}$]. This problem can be expressed as

$$\mathbf{w}(z) = \mathbf{C}(z)\mathbf{v}(z) \tag{1}$$

with the objective that

$$\mathbf{w}(z) = \mathbf{A}(z)\mathbf{u}(z). \tag{2}$$

In order to achieve this objective, a filter $\mathbf{H}(z)$ is designed that relates $\mathbf{w}(z)$ to $\mathbf{u}(z)$ according to

$$\mathbf{w}(z) = \mathbf{C}(z)\mathbf{H}(z)\mathbf{u}(z). \tag{3}$$

A solution to achieving this objective proposed by Kirkeby *et al.*[6,7] solved the problem by minimizing the cost function

$$J(z) = \mathbf{e}^{\mathrm{T}}(z^{-1})\mathbf{e}(z) + k\mathbf{v}^{\mathrm{T}}(z^{-1})\mathbf{v}(z). \tag{4}$$

The filter that minimizes this function is given by [Ref. 6, Eq. (8)]

$$\mathbf{H}(z) = (\mathbf{C}^{\mathrm{T}}(z^{-1})\mathbf{C}(z) + k\mathbf{I})^{-1}\mathbf{C}^{\mathrm{T}}(z^{-1})\mathbf{A}(z), \tag{5}$$

where k is a weighting term used to limit the energy of the transducer signal $\mathbf{v}(z)$. The solution given in Eq. (5) requires the calculation of the matrix,

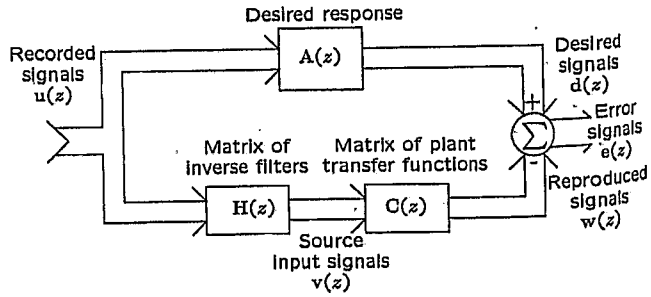

FIG. 1. Generic inverse filter system schematic (Ref. 6, Fig. 1).

 0001-4966/2006/119(1)/372/10/$22.50

$$(\mathbf{C}^{\mathrm{T}}(z^{-1})\mathbf{C}(z)+k\mathbf{I})^{-1}\mathbf{C}^{\mathrm{T}}(z^{-1}). \quad (6)$$

This matrix was observed by Elliot *et al.*[8] to be the Tikhonov inverse of the matrix $\mathbf{C}(z)$, and will hereafter be called the Tikhonov inverse filter (TIF). An extensive discussion of the Tikhonov inverse of a matrix can be found in Ref. 9. This paper will be devoted to the filter designed when $\mathbf{A}(z)=\mathbf{I}$.

Kirkeby *et al.*[6] showed that an increase in k results in an increase in the decay rate of the poles in the filter. By setting k appropriately, the length of the filters (the time at which the impulse response of the system has decayed to below the noise floor), could be reduced to fit within a finite number of points, N_{FFT}. The calculation of the filter was then possible in the frequency domain using the fast Fourier transform (FFT) without the problem of wraparound occurring when performing the inverse FFT. Calculation of the filter by this technique proved to be considerably faster than equivalent calculations performed using time domain techniques. The calculations performed in the frequency domain are given by

$$\mathbf{H}_k(\omega_i)=(\mathbf{C}^{\mathrm{H}}(\omega_i)\mathbf{C}(\omega_i)+k\mathbf{I})^{-1}\mathbf{C}^{\mathrm{H}}(\omega_i), \quad (7)$$

where $\mathbf{C}(\omega_i)$, $i\in[1,N_{\mathrm{FFT}}]$ and $\mathbf{H}_k(\omega_i)$, $i\in[1,N_{\mathrm{FFT}}]$ are the frequency domain representation of the system and Tikhonov inverse filter, respectively.

When implementing a filter design, the entire electro-acoustic system often includes sensitivities for the transmitting and receiving elements. By denoting the transmitter and receiver sensitivities as α_i, $i\in[1,N]$ and β_j, $j\in[1,M]$, respectively, the transfer matrix of the system with the sensitivities included can be expressed as

$$\begin{aligned}\mathbf{C}_{\mathrm{g}}(\omega)&=\begin{bmatrix}\beta_1 & 0 & \cdots & 0\\ 0 & \beta_2 & & \vdots\\ \vdots & & \ddots & 0\\ 0 & \cdots & 0 & \beta_{\mathrm{M}}\end{bmatrix}\\ &\quad\times\mathbf{C}(\omega)\begin{bmatrix}\alpha_1 & 0 & \cdots & 0\\ 0 & \alpha_2 & & \vdots\\ \vdots & & \ddots & 0\\ 0 & \cdots & 0 & \alpha_{\mathrm{N}}\end{bmatrix}\\ &=\boldsymbol{\beta}\mathbf{C}(\omega)\boldsymbol{\alpha}. \quad (8)\end{aligned}$$

A question raised by this form is: What influence do the sensitivities have on the resulting filters? This paper aims to address this question whereby it will be shown that the selection of $\boldsymbol{\alpha}$ and $\boldsymbol{\beta}$ to achieve the smallest condition number for $\mathbf{C}_{\mathrm{g}}(\omega)$ also decreases the high regularization that results from a poor choice of sensitivities.

In single-channel systems, the coherence between the input and the output of the system is maximized by setting the sensitivity of the transmitters to the maximum possible to reduce the noise from the electro-acoustic portion of the system, typically the largest source of noise in an acoustic system. With a multi-channel time reversal or Tikhonov inverse filter design, the level of the input signals to the electro-acoustic system is actually determined by the filter design that is developed considering both the channel and the sensitivities. If the sensitivities for each channel are set to their maximum based purely on maximizing the coherence between the input and output of the electro-acoustic system, this does not directly correspond to maximizing the coherence between the input and output of the entire system incorporating the inverse filter, the sensitivities, and the electro-acoustic system. The algorithm presented in this paper will produce the optimal set of sensitivities that provide the most balanced coherence for all channels.

III. INFLUENCE OF DIAGONAL PRECONDITIONING ON THE PERFORMANCE OF THE TIKHONOV REGULARIZED INVERSE FILTER

A. An "equally responsive system"

The influence of diagonal preconditioning on the Tikhonov inverse filter for the conditions $k=0$, and k tending toward infinity, shall be examined. The examination shall be performed for a system $\mathbf{C}(\omega)$ that is "equally responsive." A system shall be defined to be "equally responsive" when a signal transmitted from each input results in a similar level of excitation at the receivers.

When $k=0$ (i.e., no regularization) the filter created using Eq. (5) is found to be

$$\begin{aligned}\mathbf{H}(\omega)&=(\boldsymbol{\alpha}\mathbf{C}^{\mathrm{H}}(\omega)\boldsymbol{\beta}\boldsymbol{\beta}\mathbf{C}(\omega)\boldsymbol{\alpha})^{-1}\boldsymbol{\alpha}\mathbf{C}^{\mathrm{H}}(\omega)\boldsymbol{\beta}\\ &=\boldsymbol{\alpha}^{-1}(\mathbf{C}^{\mathrm{H}}(\omega)\boldsymbol{\beta}^2\mathbf{C}(\omega))^{-1}\mathbf{C}^{\mathrm{H}}(\omega)\boldsymbol{\beta}. \quad (9)\end{aligned}$$

If $\boldsymbol{\beta}=\mathbf{I}$ (i.e., equal receiver sensitivities), then Eq. (9) shows that the signal amplitude for transmitter i will be scaled by $1/\alpha_i$. The filter will thus create a set of signals that generates a higher signal level for the weaker transmitter. It then follows that the dynamic range will be fully used only for the output channel with the smallest sensitivity (assuming all the transducers have the same input dynamic range). When the matrix $\mathbf{C}$ is square, Eq. (9) can be reduced to

$$\mathbf{H}=\boldsymbol{\alpha}^{-1}(\mathbf{C}^{\mathrm{H}}(\omega)\mathbf{C}(\omega))^{-1}\mathbf{C}^{\mathrm{H}}(\omega)\boldsymbol{\beta}^{-1}, \quad (10)$$

showing that a similar attenuation is applied to the input signal according to the choice of receiver sensitivities, $\boldsymbol{\beta}$.

When regularization is included, it can be noted from Eq. (7) that as k is increased, $(\mathbf{C}_{\mathrm{g}}^{\mathrm{H}}\mathbf{C}_{\mathrm{g}}+k\mathbf{I})^{-1}$ tends toward $(1/k)\mathbf{I}$ and, as a result, the resulting filter approaches

$$\mathbf{H}(\omega)=\frac{1}{k}\mathbf{C}_{\mathrm{g}}^{\mathrm{H}}(\omega) \quad (11)$$

$$=\frac{1}{k}\boldsymbol{\alpha}\mathbf{C}^{\mathrm{H}}(\omega)\boldsymbol{\beta}, \quad (12)$$

which can be observed to be a scaled version of the frequency domain representation of the multi-channel time reversal filter.[10–12] This filter design results in the signal to transducer i being scaled by α_i, and the signal transmitted to receiver j being scaled by β_j. It then follows that the dynamic range will only be fully used for the output channel with the largest sensitivity.

It has been shown that at the two extremities of $k=0$ and $k\to\infty$ [denoted hereafter as inverse filtering (IF) and time reversal filtering (TRF)], the full dynamic range of the transducer will only be effectively used if the transducer sensitivi-

ties are equal for an "equally responsive system." It can then be noted that if the system is not equally responsive (i.e., positioning a microphone close to a pressure node), it would be desirable to find an alternative set of sensitivities that would transform the total system into an equally responsive system.

B. Influence of diagonal preconditioning on the total system

With reference to Fig. 1, the total system transfer function, being the combination of the filter and the system, is given by

$$\mathbf{T}(\omega) = \mathbf{C}(\omega)\mathbf{H}(\omega). \tag{13}$$

The influence that the transducer sensitivities have on the total system for IF and TRF can be observed by inserting Eqs. (9) and (12) into Eq. (13). The system transfer functions for IF and TRF are given by

$$\mathbf{T}_{\mathrm{IF}} = \boldsymbol{\beta}\mathbf{C}\boldsymbol{\alpha}\mathbf{H}_{\mathrm{IF}} = \boldsymbol{\beta}\mathbf{C}\boldsymbol{\alpha}((\boldsymbol{\alpha}\mathbf{C}^{\mathrm{H}}\boldsymbol{\beta}\boldsymbol{\beta}\mathbf{C}\boldsymbol{\alpha})^{-1}\boldsymbol{\alpha}\mathbf{C}^{\mathrm{H}}\boldsymbol{\beta}) = \mathbf{I} \tag{14}$$

and

$$\mathbf{T}_{\mathrm{TRF}} = \boldsymbol{\beta}\mathbf{C}\boldsymbol{\alpha}\mathbf{H}_{\mathrm{TR}} = \boldsymbol{\beta}\mathbf{C}\boldsymbol{\alpha}(\boldsymbol{\alpha}\mathbf{C}^{\mathrm{H}}\boldsymbol{\beta}) = \boldsymbol{\beta}\left(\sum_{i=1}^{\mathrm{N}} \alpha_i^2 \begin{bmatrix} c_{1i} \\ c_{2i} \\ \vdots \end{bmatrix} [c_{1i}^* \quad c_{2i}^* \quad \cdots]\right)\boldsymbol{\beta}, \tag{15}$$

respectively, and the matrix

$$\begin{bmatrix} c_{1i} \\ c_{2i} \\ \vdots \end{bmatrix} [c_{1i}^* \quad c_{2i}^* \quad \cdots] \tag{16}$$

is the transfer matrix due to the ith transmitter. It is thus observed that the variation of the transducer sensitivities have no influence on the total response for an IF but considerable influence on the TRF.

Considering that $\mathbf{C}^{\mathrm{H}}\mathbf{C}$ is diagonally dominant,[13] Eq. (15) shows that the transducer sensitivities $\boldsymbol{\beta}$ result in the signal at the jth receiver being scaled by β_j^2, and the sensitivities $\boldsymbol{\alpha}$ result in the scaling of the ith transfer matrix by α_i^2. Since the Tikhonov inverse filter has a nonzero regularization parameter, it is considered reasonable to assume that the transmission channels would also be unequally scaled.

C. Examination of the transfer matrix according to the singular values

In this section, the influence of the transducer sensitivities on the TIF will be examined according to the singular values decomposition (SVD) of the system matrix, given by

$$\mathbf{C}(\omega) = \mathbf{U}(\omega)\boldsymbol{\Sigma}(\omega)\mathbf{V}^{\mathrm{H}}(\omega) = \sum_{i=1}^{N} \sigma_i \mathbf{u}_i(\omega)\mathbf{v}_i^{\mathrm{H}}(\omega), \tag{17}$$

where $\mathbf{U}(\omega)$ and $\mathbf{V}(\omega)$ are unitary matrices, $\boldsymbol{\Sigma}(\omega)$ is a diagonal matrix of singular values, σ_i, $i \in [1,N]$, and $\mathbf{u}_i(\omega)$ and $\mathbf{v}_i(\omega)$ are the corresponding basis vectors within the unitary matrices. The inverse filter with no regularization can then be expressed as

$$\mathbf{H}_{\mathrm{IF}}(\omega) = \mathbf{V}(\omega)\boldsymbol{\Sigma}^{-1}(\omega)\mathbf{U}^{\mathrm{H}}(\omega) = \sum_{i=1}^{N} \frac{\mathbf{v}_i(\omega)\mathbf{u}_i^{\mathrm{H}}(\omega)}{\sigma_i} \tag{18}$$

and the addition of the regularization results in the filter

$$\mathbf{H}_{\mathrm{TIF}}(\omega) = \mathbf{V}(\omega)\boldsymbol{\Sigma}_{\mathrm{TIF}}(\omega)\mathbf{U}^{\mathrm{H}}(\omega) = \sum_{i=1}^{N} \left(\frac{\sigma_i^2}{\sigma_i^2 + k}\right) \frac{\mathbf{v}_i(\omega)\mathbf{u}_i^{\mathrm{H}}(\omega)}{\sigma_i}, \tag{19}$$

where the subscript TIF denotes Tikhonov inverse filter. In subsequent equations the frequency dependence (ω) is implied, but not shown. In Eq. (19) it can be seen that the magnitude of k compared to σ_i^2 [the singular values of $\mathbf{C}(\omega)\mathbf{C}^{\mathrm{H}}(\omega)$] determines the effectiveness of the "basis vector coupling" between $\mathbf{u}_i$ and $\mathbf{v}_i$.[14] Basis vector coupling is physically described as follows: $\mathbf{u}_i$ is considered similar to a mode shape that, when excited, results in an excitation of the receivers with a phase and amplitude, $\mathbf{v}_i$, scaled according to the coupling factor of σ_i.

When the sensitivities are included, the filter becomes

$$\mathbf{C}_{\mathrm{g}} = \boldsymbol{\beta}\mathbf{U}\boldsymbol{\Sigma}\mathbf{V}^{\mathrm{H}}\boldsymbol{\alpha} \tag{20}$$

$$= \mathbf{U}_{\mathrm{g}}\boldsymbol{\Sigma}_{\mathrm{g}}\mathbf{V}_{\mathrm{g}}^{\mathrm{H}}, \tag{21}$$

where $\mathbf{U}_{\mathrm{g}}, \mathbf{V}_{\mathrm{g}}$, and $\boldsymbol{\Sigma}_{\mathrm{g}}$ are the unitary and singular matrices of the new system. The basis vector coupling matrices, $\mathbf{u}_i\sigma_i\mathbf{v}_i^{\mathrm{H}}$, have been converted to $\boldsymbol{\beta}\mathbf{u}_i\sigma_i\mathbf{v}_i^{\mathrm{H}}\boldsymbol{\alpha}$. Since the set of vectors, $\boldsymbol{\beta}\mathbf{u}_i$, $i \in [1,\mathrm{M}]$ and $\boldsymbol{\alpha}\mathbf{v}_i$, $i \in [1,\mathrm{N}]$ (being the transformation of the original basis vectors); cannot be simply scaled to form another orthonormal set, it can be concluded that there is no trivial solution to relate the singular values of $\mathbf{C}$ to that of $\mathbf{C}_{\mathrm{g}}$.

In this work, the goal is to determine a new set of sensitivities that reduce the regularization that results from a poor choice of sensitivities. Given a fixed regularization parameter, k, Eq. (19) shows that to reduce the effect of the regularization on the singular values, sensitivities should be chosen that result in the largest singular values possible. This strategy by itself is unrealistic since the problem is unconstrained since $\boldsymbol{\alpha}$ and $\boldsymbol{\beta}$ can be chosen to scale the singular values by any desired amount, x, by using a set of scaling matrices,

$$\boldsymbol{\alpha} = x\mathbf{I}, \quad \boldsymbol{\beta} = \mathbf{I}. \tag{22}$$

It can further be shown using Eq. (19) that the change in regularization that results from the equal scaling of the sensitivities by x can equivalently be achieved by selecting a different regularization parameter, $k' = x^2k$. Thus, the objective of adjusting the sensitivities should not be to scale the singular values, but to minimize the condition number, being the ratio of the largest singular value to the smallest singular value.

D. Diagonal preconditioning

In Secs. III B and III C, two optimization techniques have been proposed, the former to achieve an equally respon-

sive system and the latter to reduce the condition number of the matrix. In the former technique, the transducer sensitivities are chosen such that every input signal to the system excites the outputs of the system with the same magnitude. This can be expressed as

$$|\boldsymbol{\beta}\mathbf{C}\boldsymbol{\alpha}\mathbf{e}_1|_2 = |\boldsymbol{\beta}\mathbf{C}\boldsymbol{\alpha}\mathbf{e}_2|_2 = \cdots = |\boldsymbol{\beta}\mathbf{C}\boldsymbol{\alpha}\mathbf{e}_N|_2, \tag{23}$$

where $|\cdot|_2$ is the norm-2 (or Euclidean length) of a vector, and the vectors $\mathbf{e}_1, \ldots, \mathbf{e}_N$ are the standard basis vectors for $\mathbb{R}_N$. This condition can be achieved by setting

$$\beta_i = 1, \qquad \alpha_j^2 = \frac{1}{\sum_{j=1}^{M} |c_{ij}|^2}. \tag{24}$$

By using this scaling, the resulting filters will equalize the signals transmitted, but not the signals received. In order to achieve equal signal levels at the receivers, a further condition can be imposed: for a simultaneous unit input on all the channels, the energy at each output is to be equal. To achieve this, a set of diagonal matrices, $\boldsymbol{\alpha}$ and $\boldsymbol{\beta}$, are chosen such that

$$r_1^2 = r_2^2 = \cdots = r_M^2, \tag{25}$$

where

$$\begin{bmatrix} r_1 \\ r_2 \\ \vdots \\ r_M \end{bmatrix} = \boldsymbol{\beta}\mathbf{C}\boldsymbol{\alpha} \begin{bmatrix} 1 \\ 1 \\ \vdots \\ 1 \end{bmatrix}. \tag{26}$$

A solution that achieves this is

$$\alpha_j = 1, \qquad \beta_i^2 = \frac{1}{\sum_{i=1}^{N} |c_{ij}|^2}. \tag{27}$$

When the conditions in Eqs. (24) and (27) are met, the system responds equally, and thus Tikhonov inverse filtering can be found to effectively use the full dynamic range of all the transducers within the system.

In Sec. III C it was shown that a suitable choice of diagonal matrices was the set that minimized the condition numbers of the system. Van der Sluis[15] discussed that minimization of the condition number could not be expected to be easily achieved, however it was shown in Ref. 15, Theorem 3.5, that the condition number of the matrix $\boldsymbol{\alpha}\mathbf{C}$ was upper bounded to be a factor of $\sqrt{m}$ from the minimum when all the rows have equal two-norms, and the condition number of $\mathbf{C}\boldsymbol{\beta}$ was upper bounded to be a factor of $\sqrt{n}$ from the minimum when all the columns have equal two-norms for an $m \times n$ matrix. From Eqs. (24) and (27), the diagonal matrices that best use the dynamic range of the transducers also results in a matrix of equal two-norm of both the row and columns. Thus the design techniques presented in Secs. III B and III C have the same solution, being that of diagonal matrices that result in $\mathbf{C}_g$ having rows and columns of equal two-norm.

Finding a set of diagonal matrices that achieve equal two-norms of both the columns and rows simultaneously is a nontrivial problem. In order to approximate such a condition, Ruiz[16] showed that an algorithm involving the iterative application of Eqs. (24) and (27) converges to a set of diagonal matrices that results in equal two-norms of both row and columns of the combined matrices. A variation of the algorithm by Ruiz[16] is proposed and used hereafter to calculate an optimal set of diagonal matrices:

Algorithm 1:

$$\hat{\mathbf{C}}^{(0)} = \mathbf{C}, \quad \boldsymbol{\beta}^{(0)} = \mathbf{I}, \quad \boldsymbol{\alpha}^{(0)} = \mathbf{I}$$

for $k=0,1,2,\ldots$, until convergence do

$$\mathbf{D}_R = \mathrm{diag}\left(\sqrt{|\mathbf{r}_i^{(k)}|_2}\right)_{i=1,\ldots,m},$$

$$\mathbf{D}_C = \mathrm{diag}\left(\sqrt{|\mathbf{c}_j^{(k)}|_2}\right)_{j=1,\ldots,n},$$

$$\hat{\mathbf{C}}^{(k+1)} = \mathbf{D}_R^{-1}\hat{\mathbf{C}}^{(k)}\mathbf{D}_C^{-1},$$

$$\boldsymbol{\beta}^{(k+1)} = \boldsymbol{\beta}^{(k)}\mathbf{D}_R^{-1}, \quad \text{and} \quad \boldsymbol{\alpha}^{(k+1)} = \boldsymbol{\alpha}^{(k)}\mathbf{D}_C^{-1},$$

where $\mathbf{r}_i^{(k)}$ and $\mathbf{c}_j^{(k)}$ are the ith row and jth column of the matrix $\hat{\mathbf{C}}^{(k)}$, respectively. For the experimental results given in Sec. IV, it was found that adequate convergence of the algorithm was reached after 20 iterations.

E. Preconditioning within the controller

So far the implementation of sensitivity compensation has only been discussed with respect to scaling within the analog domain. In this section the concept of scaling the signal within the digital domain will be presented. To develop a filter for use in the digital domain, it is observed that the filter, $\mathbf{H}_g$, is designed such that

$$[\boldsymbol{\beta}\mathbf{C}\boldsymbol{\alpha}]\mathbf{H}_g \simeq \mathbf{I}, \tag{28}$$

where the square brackets have been included to define the analog domain. It then follows that

$$\boldsymbol{\beta}^{-1}\boldsymbol{\beta}\mathbf{C}\boldsymbol{\alpha}\mathbf{H}_g \simeq \boldsymbol{\beta}^{-1}, \qquad [\mathbf{C}]\boldsymbol{\alpha}\mathbf{H}_g\boldsymbol{\beta} \simeq \mathbf{I}. \tag{29}$$

Thus an inverse filter for use in the digital domain is given by

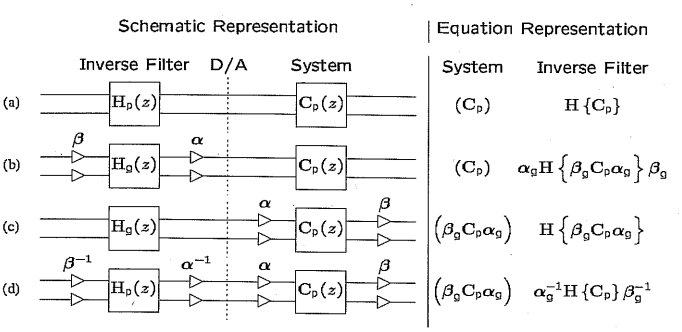

FIG. 2. Diagonal preconditioning systems: (a) no diagonal preconditioning, (b) digital preconditioning, (c) analog preconditioning, and (d) scaled version of the Tikhonov inverse filter.

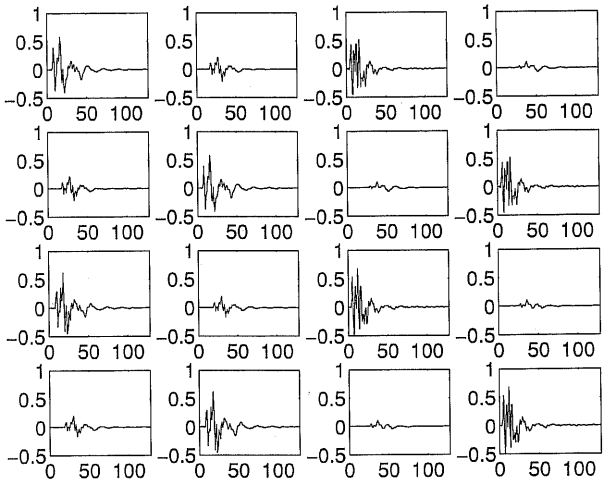

FIG. 3. The impulse responses $c_{rs}(n)$ of the system (replica of Ref. 7, Fig. 3) showing the response amplitudes versus sample, n. In this figure, the subfigure at row i, column j corresponds to the IRF of the channel between transmitter j and receiver i.

$$\mathbf{H}_{\text{digital}} = \boldsymbol{\alpha}\mathbf{H}_{\text{g}}\boldsymbol{\beta} = \boldsymbol{\alpha}((\boldsymbol{\beta}\mathbf{C}\boldsymbol{\alpha})^{\text{H}}(\boldsymbol{\beta}\mathbf{C}\boldsymbol{\alpha}) + k\mathbf{I})^{-1}(\boldsymbol{\beta}\mathbf{C}\boldsymbol{\alpha})^{\text{H}}\boldsymbol{\beta}$$
$$= (\mathbf{C}^{\text{H}}\boldsymbol{\beta}^2\mathbf{C} + k\boldsymbol{\alpha}^{-2})^{-1}\mathbf{C}^{\text{H}}\boldsymbol{\beta}^2. \quad (30)$$

The digital and analog implementations are shown in Figs. 2(b) and 2(c). When applying diagonal preconditioning in the analog domain, $\boldsymbol{\alpha}$ and $\boldsymbol{\beta}$ are chosen to transform the system $\mathbf{C}_{\text{g}}(z)$ into an equally responsive system such that the signals at the input and output of the system have relatively equal amplitudes. However, if the scaling is performed within the digital domain, the amplitude of the signals at the D/A and A/D converters are

$$\mathbf{s}_{\text{D/A}}(z) = \boldsymbol{\alpha}\mathbf{v}(z) \quad (31)$$

and

$$\mathbf{s}_{\text{A/D}}(z) = \boldsymbol{\beta}^{-1}\mathbf{w}(z), \quad (32)$$

respectively, showing that the filter does not make effective use of the D/A and A/D converters. Thus the only benefit to using diagonal preconditioning in the digital domain is to reduce the unequal regularization on the singular values that results from a poor choice of sensitivities.

IV. AN EXAMPLE ANALYSIS

In this section, a simulation will be used to demonstrate the concept of diagonal preconditioning. The simulation used is a replica of that performed by Kirkeby *et al.*[7] in which a filtering system is designed that utilizes four speakers to generate a set of desired signals at four points surrounding a dummy head. For a detailed overview of the physical configuration, see Ref. 7. The simulation utilizes transfer functions created by Gardner and Martin[17] which are freely available for download from the MIT Media Laboratory website (World Wide Web Address: http://sound.media.mit.edu/KEMAR.html). The impulse responses that describe the system are shown in Fig. 3. It should be observed that due to symmetry in the experiment, the impulse response matrix can be written in the form

$$\mathbf{C}(z) = \begin{bmatrix} c_1(n) & c_2(n) & c_3(n) & c_4(n) \\ c_2(n) & c_1(n) & c_4(n) & c_3(n) \\ c_5(n) & c_6(n) & c_7(n) & c_8(n) \\ c_6(n) & c_5(n) & c_8(n) & c_7(n) \end{bmatrix}. \quad (33)$$

It can be observed from Fig. 3 that the energies of $c_1(n)$, $c_3(n)$, $c_5(n)$, and $c_7(n)$ are relatively equal, and similarly the energies of $c_2(n)$, $c_4(n)$, $c_6(n)$, and $c_8(n)$ are relatively equal. From this it can be concluded that the norm-2 of the rows

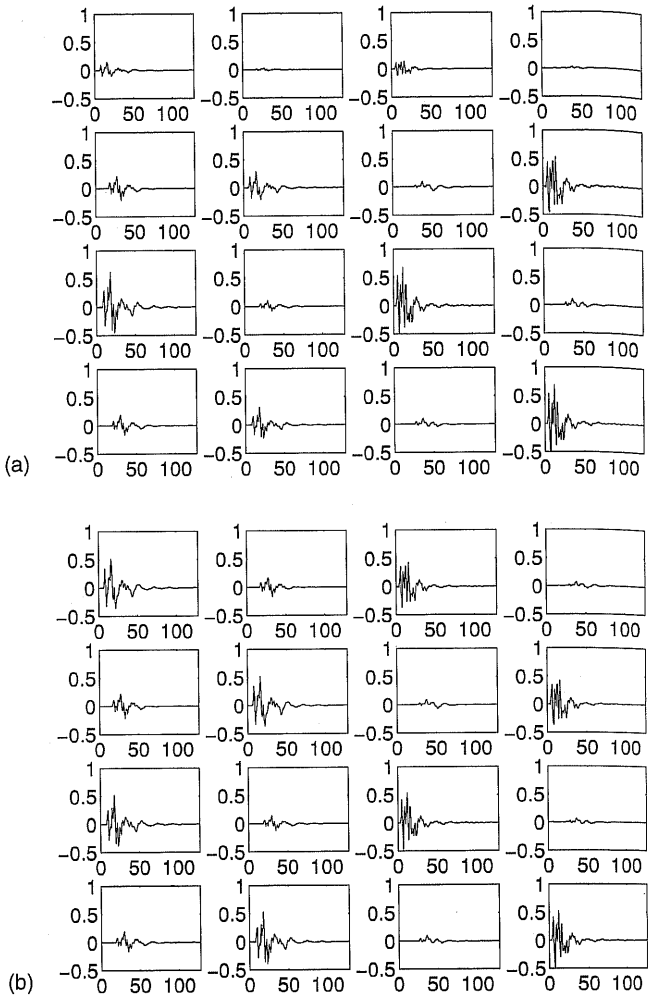

FIG. 4. The impulse responses $c(n)$. In these figures, the subplot at row i, column j corresponds to the IRF of the channel between transmitter j and receiver i. (a) Poorly scaled system, $\mathbf{C}_{\text{p}}$. (b) Poorly scaled system after application of gain compensation, $\boldsymbol{\beta}_{\text{g}}\mathbf{C}_{\text{p}}\boldsymbol{\alpha}$.

TABLE I. Energy within the rows and columns of the transfer matrices.

System	Rows	Columns
Poor scaled system ($\mathbf{C}_{\text{p}}$)	$[0.70 \quad 0.44 \quad 0.77 \quad 1.00]^{\text{T}}$	$[0.24 \quad 0.81 \quad 1.00 \quad 0.86]$
Compensated ($\boldsymbol{\beta}_{\text{g}}\mathbf{C}_{\text{p}}\boldsymbol{\alpha}_{\text{g}}$)	$[1.00 \quad 0.98 \quad 1.00 \quad 0.98]^{\text{T}}$	$[0.98 \quad 1.00 \quad 0.98 \quad 1.00]$

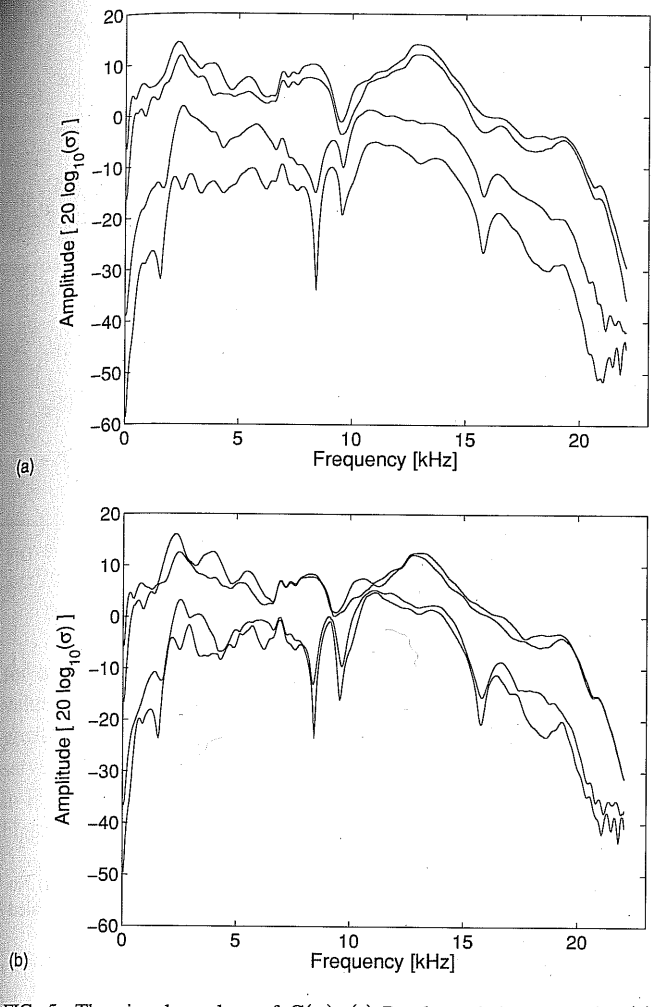

FIG. 5. The singular values of $\mathbf{C}(\omega)$. (a) Poorly scaled system, $\mathbf{C}_\mathrm{p}$. (b) Poorly scaled system after application of gain compensation, $\boldsymbol{\beta}_\mathrm{g}\mathbf{C}_\mathrm{p}\boldsymbol{\alpha}$.

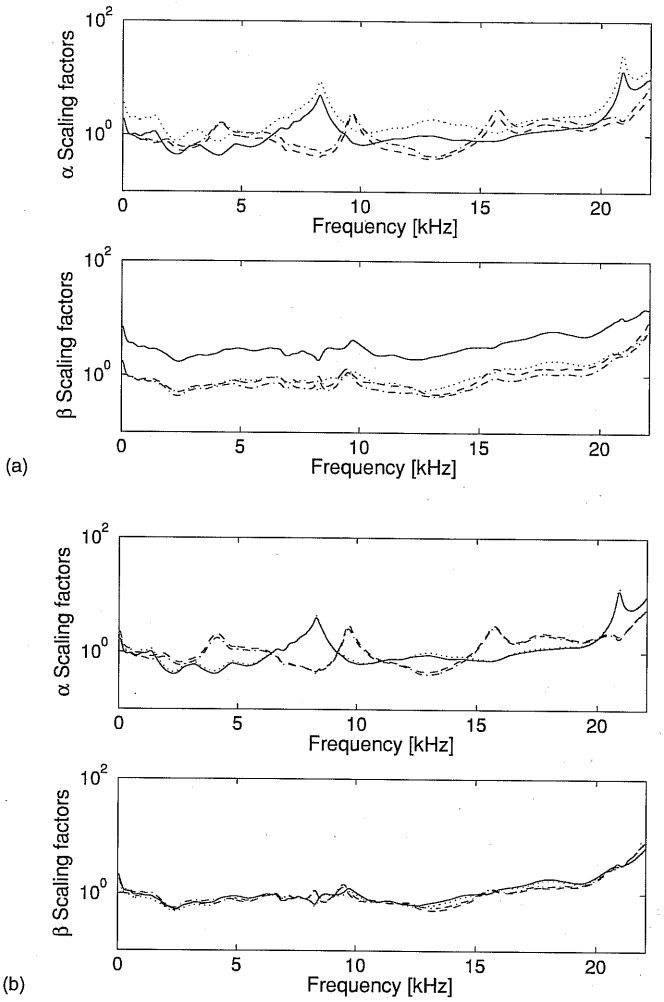

FIG. 6. Optimal values of $\boldsymbol{\alpha}$ and $\boldsymbol{\beta}$ with respect to frequency, calculated using the preconditioning algorithm; ———x_1, ···x_2, -·-·-x_3, - - -x_4, where $x=\boldsymbol{\alpha}$ and $\boldsymbol{\beta}$, respectively. (a) Poorly scaled system, $\mathbf{C}_\mathrm{p}$. (b) Poorly scaled system after application of gain compensation, $\boldsymbol{\beta}_\mathrm{g}\mathbf{C}_\mathrm{p}\boldsymbol{\alpha}$.

and columns of this matrix are likely to be fairly similar, and thus the system is equally responsive. To examine the influence of diagonal preconditioning, a set of gains will be used to cause the system to be poorly scaled, and then, to demonstrate the proposed technique, a set of gains will be calculated using Algorithm 1 to compensate for the poor scaling.

The set of gains arbitrarily chosen to create a system with a poor choice of sensitivities is given by

$$\boldsymbol{\alpha}_\mathrm{p}=\begin{bmatrix}1.00 & 0 & 0 & 0\\ 0 & 0.50 & 0 & 0\\ 0 & 0 & 1.00 & 0\\ 0 & 0 & 0 & 1.00\end{bmatrix},$$

$$\boldsymbol{\beta}_\mathrm{p}=\begin{bmatrix}0.25 & 0 & 0 & 0\\ 0 & 1.00 & 0 & 0\\ 0 & 0 & 1.00 & 0\\ 0 & 0 & 0 & 1.00\end{bmatrix}, \tag{34}$$

with the resulting IRFs shown in Fig. 4(a). This system will be denoted as $\mathbf{C}_\mathrm{p}$, where the subscript p denotes *poorly scaled*. The scaling introduced physically corresponds to transmitter 2 having half the sensitivity of the other transmitters and receiver 1 having a sensitivity a quarter that of the other elements. A set of compensating gains was then calculated by applying Algorithm 1 to the system energy matrix,

$$\mathbf{E}=\begin{bmatrix}\sqrt{\sum_n c_{11}^2(n)} & \sqrt{\sum_n c_{12}^2(n)} & \sqrt{\sum_n c_{13}^2(n)} & \sqrt{\sum_n c_{14}^2(n)}\\ \sqrt{\sum_n c_{21}^2(n)} & \sqrt{\sum_n c_{22}^2(n)} & \sqrt{\sum_n c_{23}^2(n)} & \sqrt{\sum_n c_{24}^2(n)}\\ \sqrt{\sum_n c_{31}^2(n)} & \sqrt{\sum_n c_{32}^2(n)} & \sqrt{\sum_n c_{33}^2(n)} & \sqrt{\sum_n c_{34}^2(n)}\\ \sqrt{\sum_n c_{41}^2(n)} & \sqrt{\sum_n c_{42}^2(n)} & \sqrt{\sum_n c_{43}^2(n)} & \sqrt{\sum_n c_{44}^2(n)}\end{bmatrix}. \tag{35}$$

The resulting compensation gains are

$$\boldsymbol{\alpha}_\mathrm{g}=\begin{bmatrix}1.06 & 0 & 0 & 0\\ 0 & 1.85 & 0 & 0\\ 0 & 0 & 0.99 & 0\\ 0 & 0 & 0 & 0.83\end{bmatrix},$$

$$\boldsymbol{\beta}_\mathrm{g}=\begin{bmatrix}3.30 & 0 & 0 & 0\\ 0 & 0.96 & 0 & 0\\ 0 & 0 & 0.79 & 0\\ 0 & 0 & 0 & 0.93\end{bmatrix}. \tag{36}$$

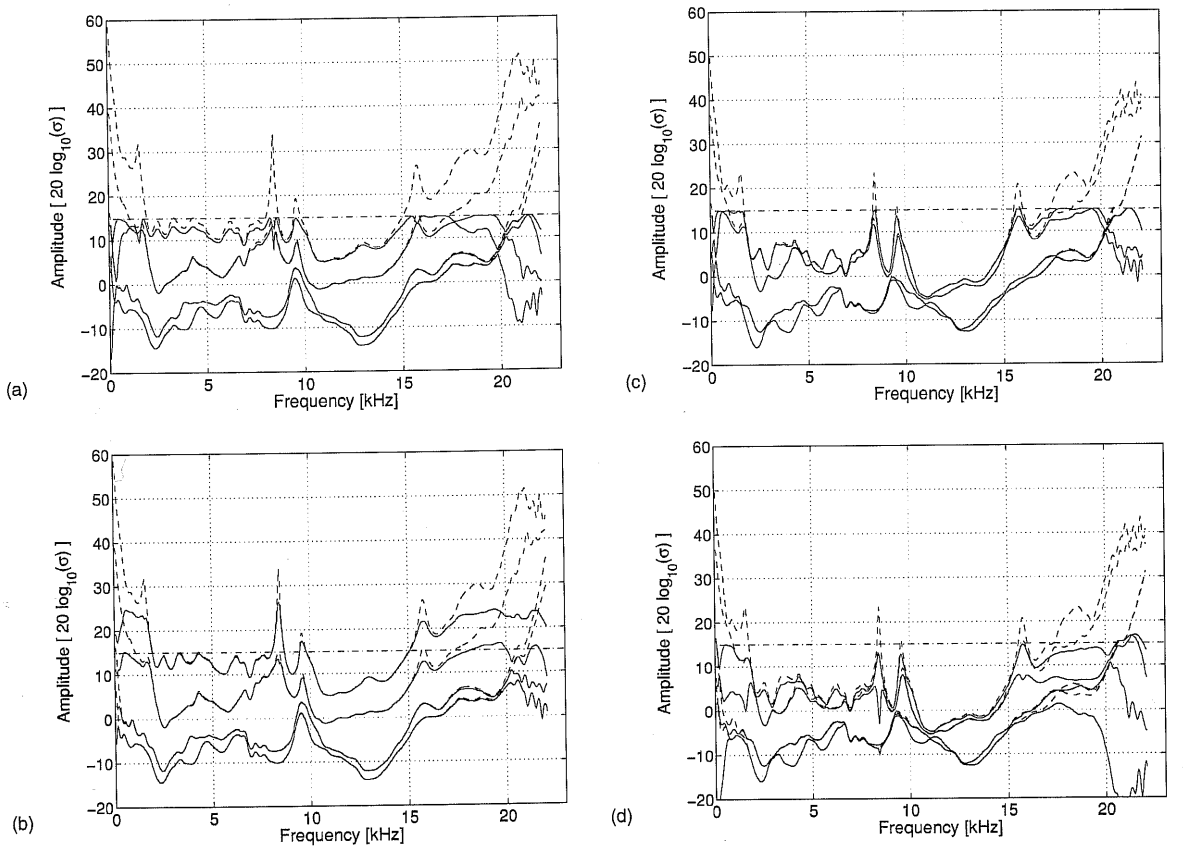

FIG. 7. The singular values of the $\mathbf{H}_{\mathrm{TIF}}(\omega_n)$ for k=0.008, ———with regularization; - - - without regularization, ····· singular value limit, $1/2\sqrt{k}$. (a) No preconditioning, $\mathbb{H}\{\mathbf{C}_\mathrm{p}\}$. (b) Digital preconditioning, $\boldsymbol{\alpha}_\mathrm{g}^{-1}\mathbb{H}\{\boldsymbol{\beta}_\mathrm{g}\mathbf{C}_\mathrm{p}\boldsymbol{\alpha}_\mathrm{g}\}\boldsymbol{\beta}_\mathrm{g}^{-1}$. (c) Analog preconditioning, $\mathbb{H}\{\boldsymbol{\beta}_\mathrm{g}\mathbf{C}_\mathrm{p}\boldsymbol{\alpha}_\mathrm{g}\}$. (d) No preconditioning, scaled $\boldsymbol{\alpha}_\mathrm{g}^{-1}\mathbb{H}\{\mathbf{C}_\mathrm{p}\}\boldsymbol{\beta}_\mathrm{g}^{-1}$.

Figure 4(b) shows the IRFs of the system after sensitivity compensation has been applied (i.e., the application of $\boldsymbol{\alpha}_\mathrm{p}\boldsymbol{\alpha}_\mathrm{g}$ and $\boldsymbol{\beta}_\mathrm{p}\boldsymbol{\beta}_\mathrm{g}$ to the initial system.) Table I shows the energy within the rows and columns of both systems, normalized such that the largest energy level is unity. As the energy within each row and each column for the sensitivity-compensated system are of similar magnitude (in contrast to that of the poorly scaled system), the algorithm is thus observed to work as desired.

The singular values of the two systems as a function of frequency are shown in Fig. 5. It can be observed in this figure that when the system is poorly scaled, the spread of the singular values is much larger than that obtained when compensation gains are used.

Figure 6 shows the sensitivities, $\boldsymbol{\alpha}$ and $\boldsymbol{\beta}$, that would result in the optimal scaling for each particular frequency. It can be observed that with gain compensation, the spread of these curves is reduced. If the system is to be used for band-limited operation, then in practice a choice of sensitivities would be found by averaging the $\boldsymbol{\alpha}$ and $\boldsymbol{\beta}$ over the desired bandwidth of operation.

In Sec. III E it was shown that diagonal preconditioning could be performed in either the digital or analog domain. To understand the results obtained using diagonal preconditioning, various forms of diagonal preconditioning shall be examined, and these are illustrated in Fig. 2. In order to compare the performance of the filter with and without diagonal preconditioning, the system that the filters are compensating for should be identical. Figure 2 shows that when diagonal preconditioning is implemented in the digital domain [Fig. 2(b)], the system being compensated is the same as that for the implementation without preconditioning [Fig. 2(a)]. However, when diagonal preconditioning is implemented in the analog domain [Fig. 2(c)], the system being compensated is different. In order to have a benchmark against which the performance of the analog implementation can be compared, a new filter has been introduced, being the Tikhonov inverse filter formed from the system with no preconditioning scaled for a system with poor sensitivities using the same method and assumptions used to obtain Eq. (30). This filter is shown in Fig. 2(d).

The singular value curves of the filters presented in Fig. 2 are shown in Fig. 7. These curves represent the "basis vector coupling" discussed in Sec. III C. Figures 7(a) and 7(b) show the singular values of the filters that are designed to compensate for the coupling in Fig. 5(a), while Fig. 7(c) and 7(d) show the singular values of the filters designed to compensate for the coupling represented in Fig. 5(b).

Figures 7(a) and 7(c) show that the filters do not have any singular values that exceed 15 dB. This limit can be explained with reference to Eqs. (18) and (19) where regularization changes the singular value from $1/\sigma_i$ to $\sigma_i^2/(\sigma_i^2+k)\sigma_i$. A plot of these functions is given in Fig. 8 for k=0.008. In this figure, the regularization is observed to limit the singular value to 15 dB. In the Appendix it is shown that

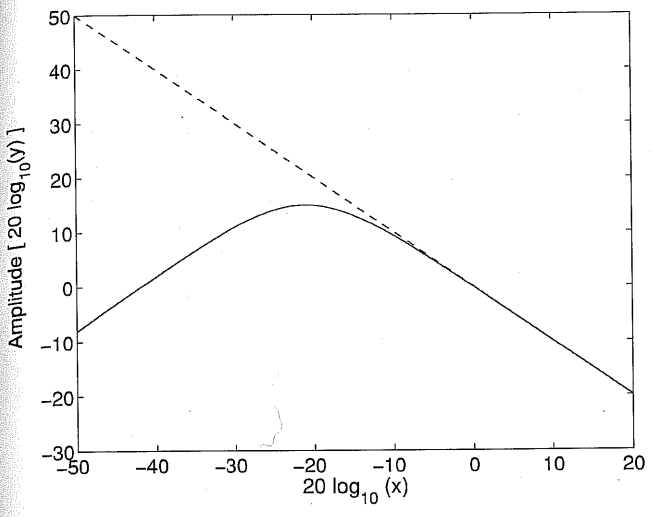

FIG. 8. Influence of regularization of singular values; - - - $y=1/x$, ——— $y=x^2/(x^2+0.008)x$.

for a regularization parameter of k, the maximum singular value possible is $1/2\sqrt{k}$, obtained when $\sigma_i=\sqrt{k}$. When σ_i is greater than $\sqrt{k}$, the singular values of the filter can be observed to mirror about $1/2\sqrt{k}$ as in Fig. 8. This limit is shown in Fig. 7 and is labeled the singular value limit. Comparing Figs. 7(a) and 7(b), it is observed that the singular values are no longer limited at 15 dB, but rather a regularization is evident that takes into account the poor choice of sensitivities in the system.

Figures 7(b) and 7(d) show the singular value curves of the filter designed for a system with appropriately chosen sensitivities for the transducers. Comparing these two filters, it can be observed that the filter designed using poor sensitivities [Fig. 7(d)] has been regularized considerably compared to the filter designed for a correctly scaled system [Fig. 7(b)]. This regularization is visible on the lowest curve above 15 kHz, where such heavy regularization is unwarranted.

Figure 9 shows the resulting IRFs of the filter when the filters are normalized such that the largest peak is ±1. By implementing diagonal preconditioning in the analog domain [Fig. 9(c)], the amplitude of the IRFs are fairly similar, resulting in better use of the dynamic range of the transducers, whereas when diagonal preconditioning is implemented in the digital domain, the magnitude of the IRFs suffer as they are required to compensate for the poor sensitivities given by Eq. (34). Figure 9(d) shows the system response obtained when the filter is designed using poor sensitivities and scaled to be implemented for a system with a better choice of sensitivities. The filter is observed to make poor use of the channels compared to the filter [Fig. 9(c)] designed with correct

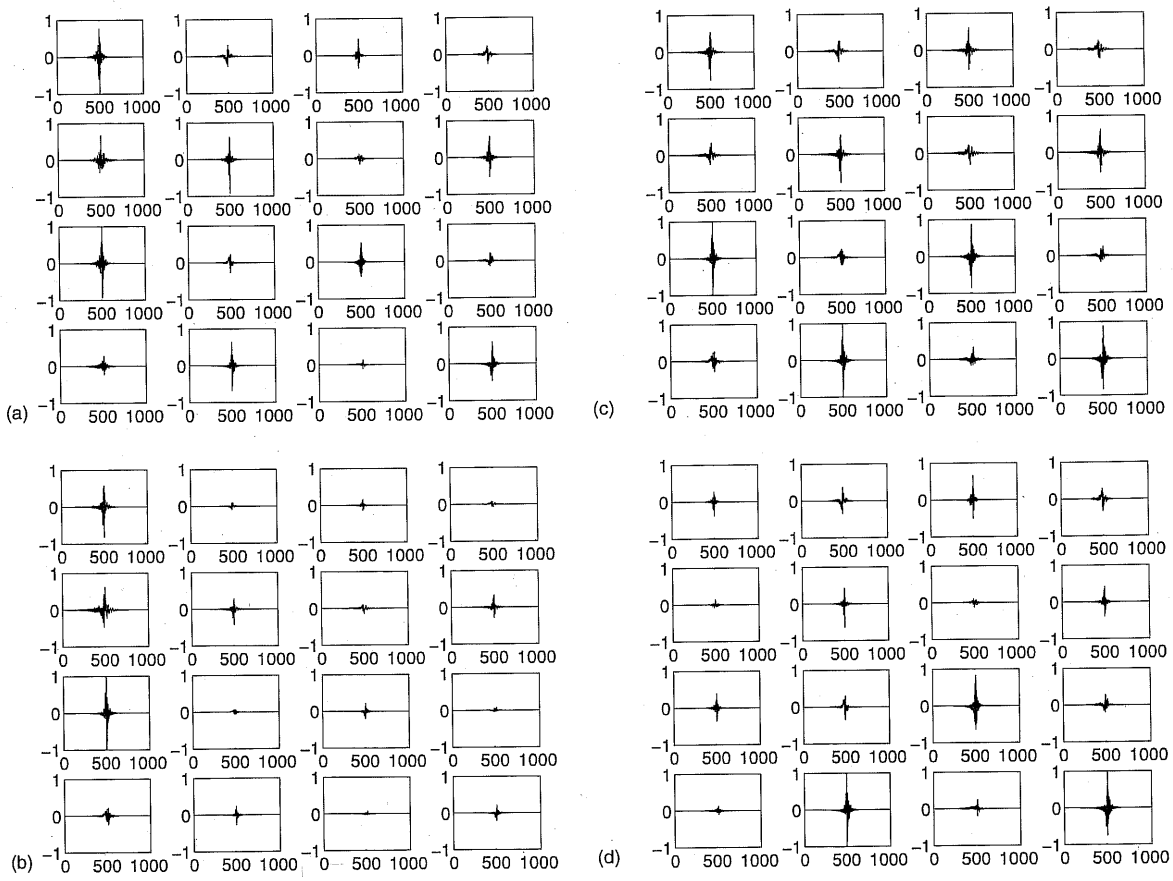

FIG. 9. The impulse responses of the filters for $k=0.008$. The unit on the x axis is samples. In these figures, the subplot at row i, column j corresponds to the IRF of the filter between virtual source j and transmitter i. These impulse responses have been normalized such that the largest peak value of each filter is ±1. (a) No preconditioning, $\mathbb{H}\{\mathbf{C}_p\}$. (b) Digital preconditioning, $\boldsymbol{\alpha}_g^{-1}\mathbb{H}\{\boldsymbol{\beta}_g\mathbf{C}_p\boldsymbol{\alpha}_g\}\boldsymbol{\beta}_g^{-1}$. (c) Analog preconditioning, $\mathbb{H}\{\boldsymbol{\beta}_g\mathbf{C}_p\boldsymbol{\alpha}_g\}$. (d) No preconditioning, scaled $\boldsymbol{\alpha}_g^{-1}\mathbb{H}\{\mathbf{C}_p\}\boldsymbol{\beta}_g^{-1}$.

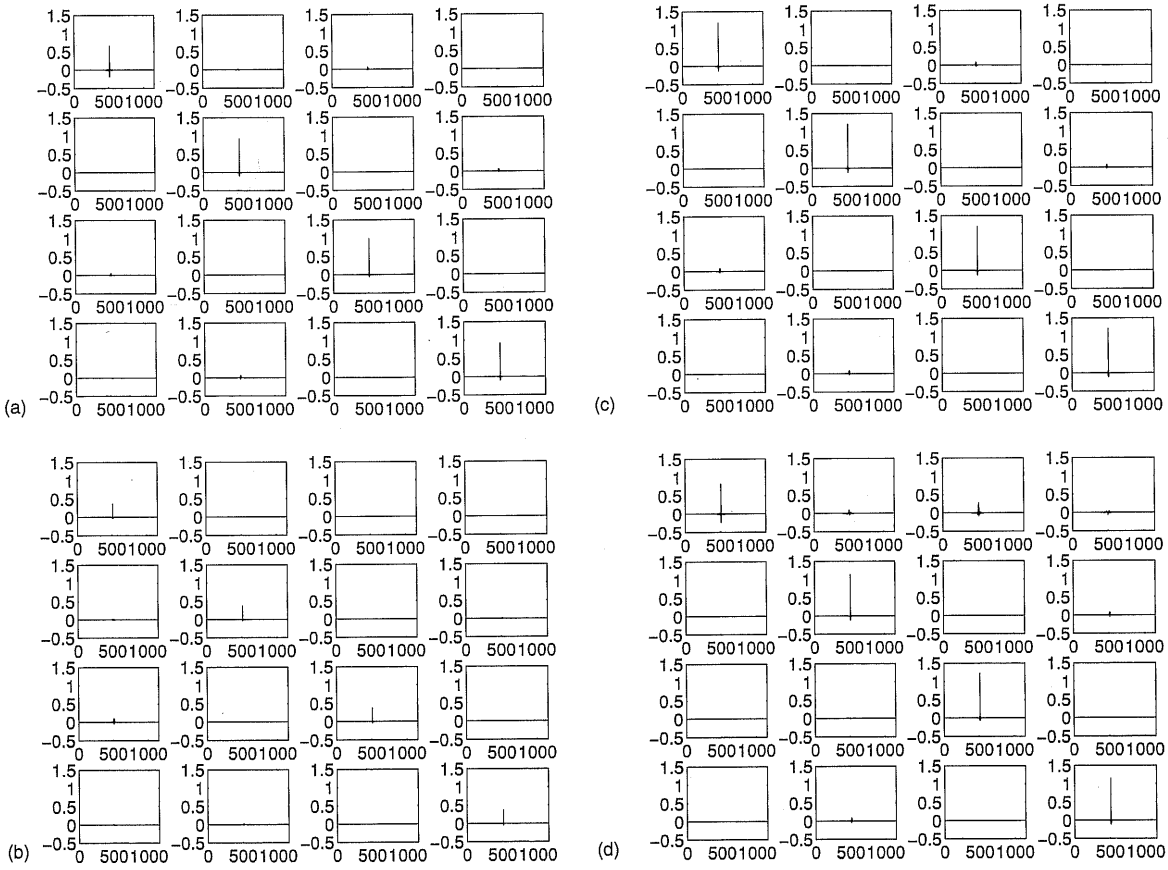

FIG. 10. The impulse responses of the complete system for $k=0.008$. The unit on the x axis is samples. In this figure, the subplot at row i, column j corresponds to the IRF of the entire system between virtual source j and receiver i. (a) No preconditioning, $\mathbb{H}\{\mathbf{C}_p\}$. (b) Digital preconditioning, $\boldsymbol{\alpha}_g^{-1}\mathbb{H}\{\boldsymbol{\beta}_g\mathbf{C}_p\boldsymbol{\alpha}_g\}\boldsymbol{\beta}_g^{-1}$. (c) Analog preconditioning, $\mathbb{H}\{\boldsymbol{\beta}_g\mathbf{C}_p\boldsymbol{\alpha}_g\}$. (d) No preconditioning, scaled $\boldsymbol{\alpha}_g^{-1}\mathbb{H}\{\mathbf{C}_p\}\boldsymbol{\beta}_g^{-1}$.

sensitivities. Applying scaling to compensate for transducer sensitivities is thus not as effective as setting the transducer sensitivities to the optimal values.

Figure 10 shows the IRFs of the entire system from the desired signal, $\mathbf{u}(z)$, to the received signal, $\mathbf{w}(z)$, using the filters shown in Fig. 9. In Fig. 10(a) it is observed that because of the effort required to transmit to receiver 1 the regularization has reduced the quality of the response and also the level of the signal received. When the sensitivities obtained using Algorithm 1 are used [Figs. 10(b) and 10(c)], it is observed that the magnitude of the pulse and the quality are much more similar over all the channels. The implementation of diagonal preconditioning in the digital domain [Fig. 10(b)] is shown to have a better response across all receivers at the cost of reducing the signal level. Figure 10(d) shows the system response obtained when the filter is designed using poor sensitivities and scaled to be implemented for a system with a better choice of sensitivities. It can be observed that the performance of this filter is much worse than that given in Fig. 10(c), being the filter designed for the properly scaled system.

Figure 11 shows the frequency response functions (FRFs) of the entire system from the desired signal to be received, $\mathbf{u}(z)$, to the actual signal received, $\mathbf{w}(z)$, using the filters shown in Figs. 9(a) and 9(c). The system response of Figs. 9(b) and 9(d) have not been included, as they have very similar spectra to the filters shown in Figs. 9(c) and 9(a), respectively. Comparing Figs. 11(a) and 11(b), the frequency response at the first receiver is noticeably improved with little change observed in the cross-talk cancellation, observable in the off-diagonal FRFs.

V. CONCLUSION

In this paper it has been demonstrated that the choice of sensitivities used within the amplifying stages of an acoustic system can have a significant influence on the performance of a filter designed using the Tikhonov inverse filtering method. An algorithm has been presented that generates a set of gains that can compensate for poorly selected receiver and transmitter sensitivities. It has been shown that improvements in performance can be obtained by using the compensated sensitivities.

ACKNOWLEDGEMENT

Thanks are given to Professor Phillip Nelson who provided an insightful conversation in regards to the Tikhonov inverse filtering.

APPENDIX: MAXIMUM SINGULAR VALUE OF A TIKHONOV INVERSE FILTER

In Sec. III C it was shown that the addition of Tikhonov regularization changes the singular values of the filter from

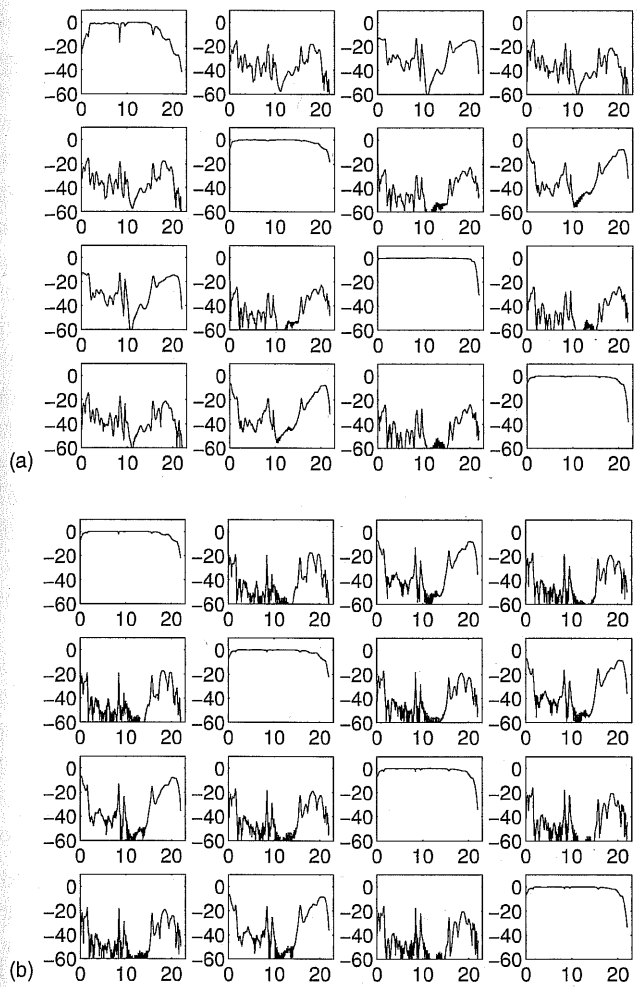

FIG. 11. The frequency responses of the complete system for $k=0.008$. The unit on the abscissa is kHz, and the unit on the ordinate is dB. In these figures, the subplot at row i, column j corresponds to the FRF of the entire system between virtual source j and transmitter i.

$$\sigma_{\mathrm{IF}} = \frac{1}{\sigma_i} \tag{A1}$$

to

$$\sigma_{\mathrm{TIF}} = \frac{\sigma_i^2}{(\sigma_i^2 + k)\sigma_i}. \tag{A2}$$

Figure 8 shows a plot of these two functions when $k=0.008$. In this figure, the singular values are observed to be limited to 15 dB. The maximum singular value for any k can be found by determining σ_{TIF} when $(\partial/\partial\sigma_i)\sigma_{\mathrm{TIF}}=0$, where

$$\frac{\partial}{\partial\sigma_i}\sigma_{\mathrm{TIF}} = \frac{1}{(\sigma_i^2 + k)} - \frac{2\sigma_i^2}{(\sigma_i^2 + k)^2} = \frac{(\sigma_i^2 + k) - 2\sigma_i^2}{(\sigma_i^2 + k)^2} \tag{A3}$$

Setting $(\partial/\partial\sigma_i)\sigma_{\mathrm{TIF}}=0$,

$$(\sigma_i^2 + k) - 2\sigma_i^2 = 0,$$

$$\sigma_i = \sqrt{k}. \tag{A4}$$

Inserting σ_i into Eq. (A2), we obtain

$$\sigma_{\mathrm{TIF}} = \frac{1}{2\sqrt{k}}. \tag{A5}$$

[1]Y. Kim and P. A. Nelson, "Spatial resolution limits for the reconstruction of acoustic source strength by inverse methods," J. Sound Vib. **265**, 583–608 (2003).

[2]J. Mourjopoulos, "On the variation and invertibility of room impulse response functions," J. Sound Vib. **102**, 217–228 (1985).

[3]S. Neely and J. Allen, "Invertibility of a room impulse response," J. Acoust. Soc. Am. **66**, 165–169 (1979).

[4]P. A. Nelson, F. Orduña Bustamante, and H. Hamada, "Inverse filter design and equalization zones in multichannel sound reproduction," IEEE Trans. Speech Audio Process. **3**, 185–192 (1995).

[5]P. Roux and M. Fink, "Time reversal in a waveguide: Study of the temporal and spatial focusing," J. Acoust. Soc. Am. **107**, 2418–2429 (2000).

[6]I. Kirkeby, P. Nelson, H. Hamada, and F. Orduña Bustamante, "Fast deconvolution of multi-channel systems using regularisation," Technical Report 255, Institute of Sound and Vibration Research, Southhampton S017 1BJ, England (1996).

[7]O. Kirkeby, P. Nelson, H. Hamada, and F. Orduña Bustamante, "Fast deconvolution of multichannel systems using regularization," IEEE Trans. Speech Audio Process. **6**, 189–195 (1998).

[8]S. J. Elliot, C. C. Boucher, and P. A. Nelson, "The behaviour of a multiple channel active control system," IEEE Trans. Signal Process. **40**, 1042–1052 (1992).

[9]P. C. Hansen, *Rank-Deficient and Discrete Ill-Posed Problems: Numerical Aspects of Linear Inversion, SIAM Monographs on Mathematical Modeling and Computation* (Society for Industrial and Applied Mathematics, Philadelphia, PA, 1998).

[10]D. Jackson and D. Dowling, "Phase conjugation in underwater acoustics," J. Acoust. Soc. Am. **89**, 171–181 (1991).

[11]W. A. Kuperman, W. S. Hodgkiss, H. C. Song, T. Akal, C. Ferla, and D. R. Jackson, "Phase conjugation in the ocean: Experimental demonstration of an acoustic time-reversal mirror," J. Acoust. Soc. Am. **103**, 25–40 (1998).

[12]C. Prada, S. Manneville, D. Spoliansky, and M. Fink, "Decomposition of the time reversal operator: Detection and selective focusing on two scatterers," J. Acoust. Soc. Am. **99**, 2067–2076 (1996).

[13]M. Tanter, J.-L. Thomas, and M. Fink, "Time reversal and the inverse filter," J. Acoust. Soc. Am. **108**, 223–234 (2000).

[14]M. Tanter, J.-F. Aubry, J. Gerber, J.-L. Thomas, and M. Fink, "Optimal focusing by spatio-temporal inverse filter. I. Basic principles," J. Acoust. Soc. Am. **110**, 37–47 (2001).

[15]A. Van der Sluis, "Condition numbers and equilibration of matrices," Numer. Math. **14**, 14–23 (1969).

[16]D. Ruiz, "A scaling algorithm to equilibrate both rows and columns norms in matrices," Technical Report RAL-TR-2001-034, Rutherford Appleton Laboratory (2001).

[17]B. Gardner and K. Martin, "HRTF measurements of a KEMAR dummy-head microphone," Technical Report 280, MIT Media Lab Perceptual Computing, MIT Media Lab, E15-401D, Cambridge, MA 02139 (1994).